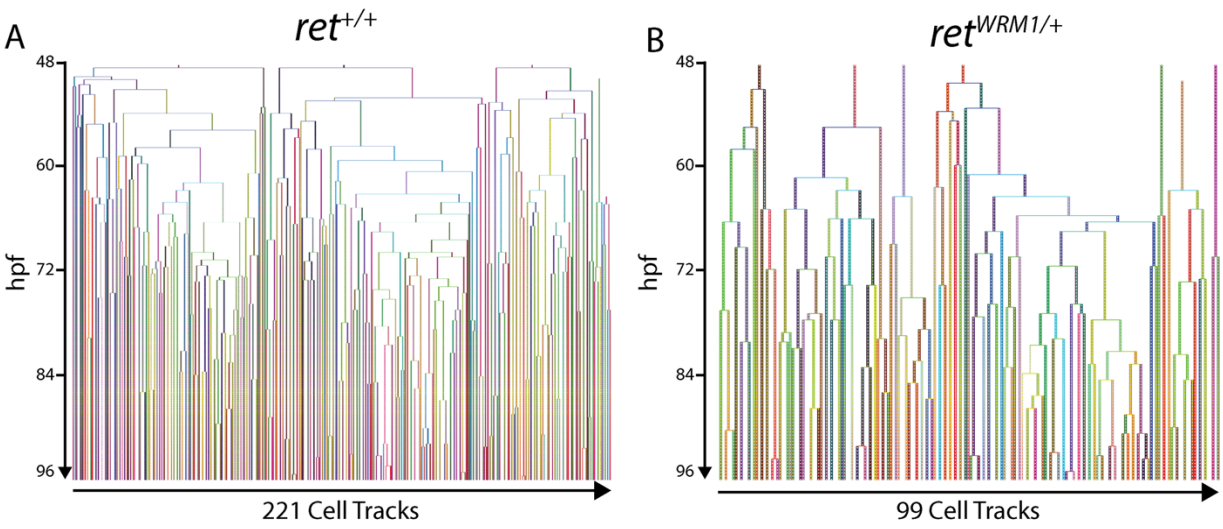

Fig. S1. IMARIS snapshots of ENCC generation trees from representative 48-96 hpf time-lapses. (A) *ret*$^{+/+}$ ENCC generation tree reveals emergence of 221 ENCCs between 48-96 hpf. (B) *ret*$^{wmr1/+}$ ENCC generation tree reveals emergence of 99 ENCCs between 48-96 hpf.

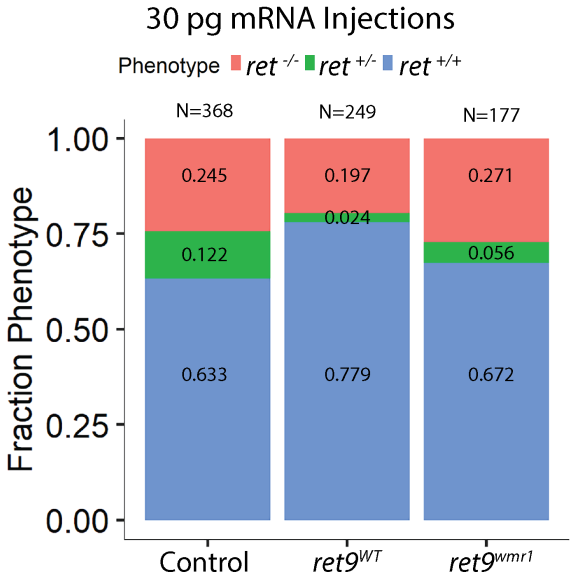

Fig. S2. *ret*^{WT} mRNA partially rescues the percentage of HSCR phenotypes seen in larvae from a *ret*$^{wmr1/+}$ incross. Stacked bar graphs depict fraction of *ret*$^{+/+}$ (WT; Blue), *ret*$^{+/-}$ (HSCR-like; Green) and *ret*$^{-/-}$ (Total Agangionosis; Magenta) phenotypes scored in *ret*$^{wmr1/+}$ incross F2's at 96 hpf following uninjected control, 30 pg *ret9*^{WT} mRNA and 30 pg *ret9*^{wmr1} mRNA. *ret9*^{WT} mRNA shows partial rescue of disease phenotypes while *ret9*^{wmr1} mRNA fails to rescue, demonstrating loss-of-function.

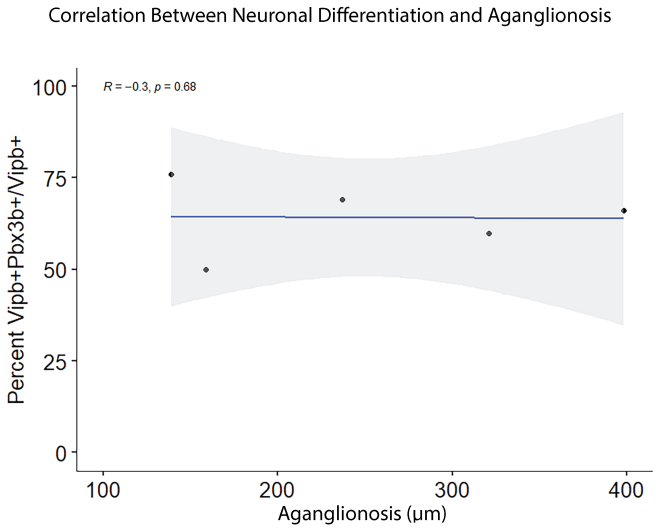

Fig. S3. No correlation between *pbx3b*$^{+}$ enteric neuronal differentiation and extent of aganglionosis in *ret*$^{wmr1/+}$ larvae at 96 hpf. *ret*$^{wmr1/+}$ larvae used in figure 6G were analyzed to measure the distance between distal most *vipb*$^{+}$ ENCCs and cloaca (Aganglionosis (*μ*m)). Scatter plot depicting percent *pbx3b*$^{+}$ (*vipb*$^{+}$*pbx3b*$^{+}$*/vipb*$^{+}$) vs extent of aganglionosis (*μ*m) tested using Spearman correlation (*R*=-0.3) finds no correlation between the two variables.

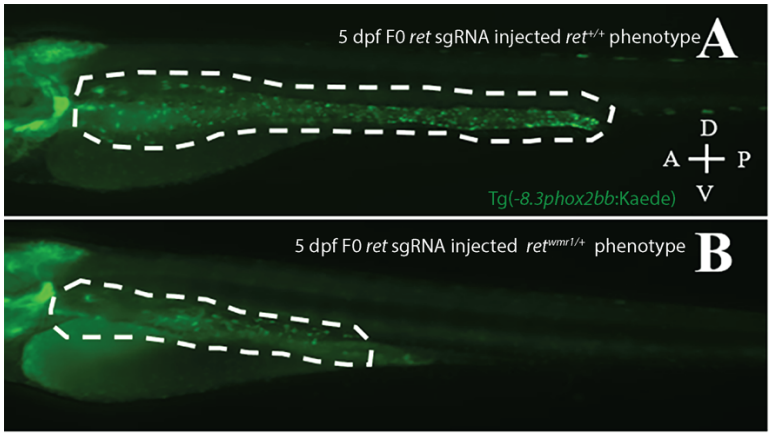

Fig. S4. Phenotypic crispant screen of F0 *ret* sgRNA injected Tg(*-8.3phox2bb:*Kaede) larvae. (A) 5 dpf *ret* sgRNA injected Tg(*-8.3phox2bb:*Kaede) larvae exhibiting *ret*$^{+/+}$ phenotype with Kaede^{+} ENCCs throughout the gut. (B) 5 dpf *ret* sgRNA injected Tg(*-8.3phox2bb:*Kaede) larvae exhibiting *ret*$^{wmr1/+}$ phenotype lacking Kaede^{+} ENCCs throughout the hindgut. Gut tube colonized by ENCCs outlined by white dashed lines. A: anterior; P: posterior; D: dorsal; V: ventral, shown in A.

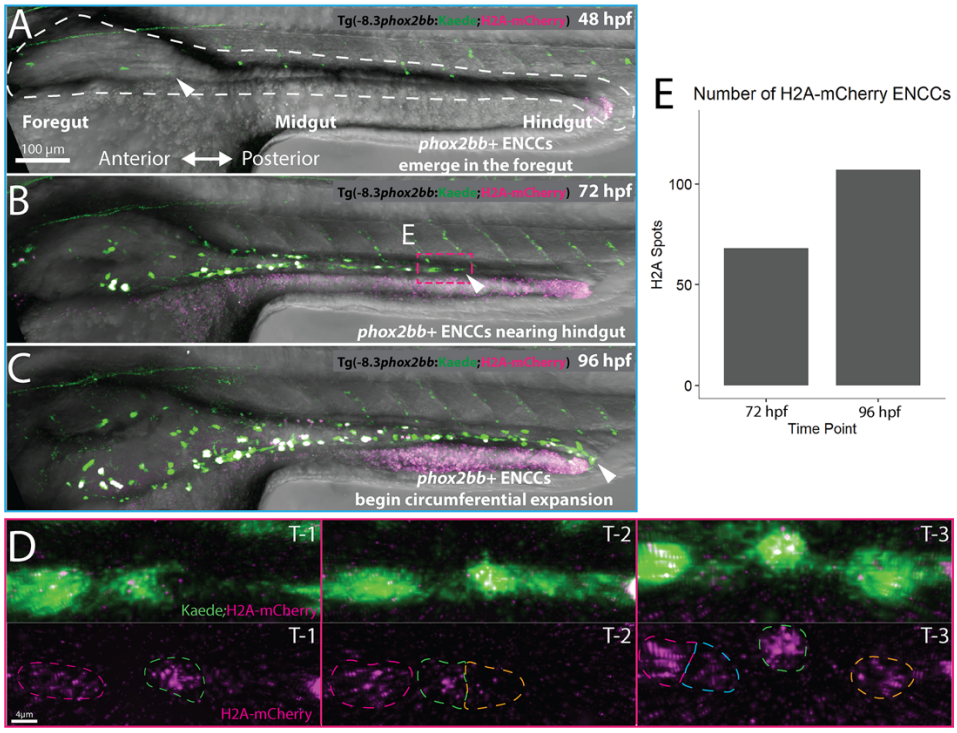

Fig. S5. 4D time-lapse microscopy between 48-96 hpf in transgenic line Tg(-8.3*phox2bb*:Kaede;H2A-mCherry). (A-C) Still images from time-lapse reveal (A, white arrow) *phox2bb*+ ENCCs emerging in foregut intestine at 48hpf (B, white arrow), leading ENCCs reaching the hindgut at 72 hpf (C), and the circumferential expansion of ENCCs at 96 hpf. (D) Expanded images of cell migration and division at the ENCC wavefront seen in panel B, magenta box. Time-points 1-3 (T1-3) depict representative time-points where cell divisions occur. (E) Quantifications of H2A-mCherry+ cells at 72 and 96 hpf reveal comparable ENCCs number to *ret*$^{wmr1/+}$ *phox2bb*:Kaede cell counts (Fig. 3A).

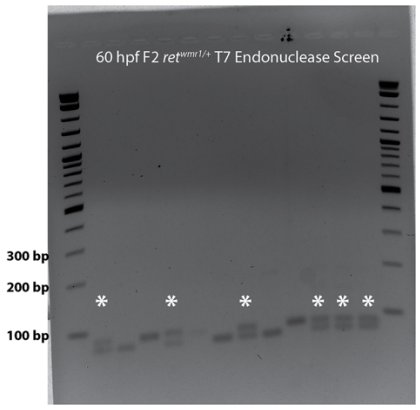

Fig. S6. T7 endonuclease assay identifies *ret*$^{wmr1/+}$ genotype in 60 hpf F2 larvae. 3% agarose gel used to separate T7 endonuclease cleaved PCR product of *ret* loci identifies heterozygotic *ret*$^{wmr1/+}$ larvae (starred lanes) from genomic DNA isolated from dissected heads. Heterozygotic larvae collected and pooled for fixed tissue hybridization chain reaction and whole-mount immunofluorescence assays.

Table S1. Phenotypic scores of 5 dpf F2 embryos obtained from *ret*$^{wmr1/+}$ in-cross. Table shows total counts and percent prevalence of *ret*$^{+/+}$ (WT), *ret*$^{wmr1/+}$ (HSCR-like), and *ret*$^{wm1/wmr1}$ (Total aganglionosis) embryos.

Plate		F2 Ret$^{WMR1/+}$
"WT Phenotype" (+/+)	Counts	32
	Percent	16.93
HSCR Phenotype (-/+)	Counts	53
	Percent	28.04
No Cells in ENS (-/-)	Counts	104
	Percent	55.03
Total		189

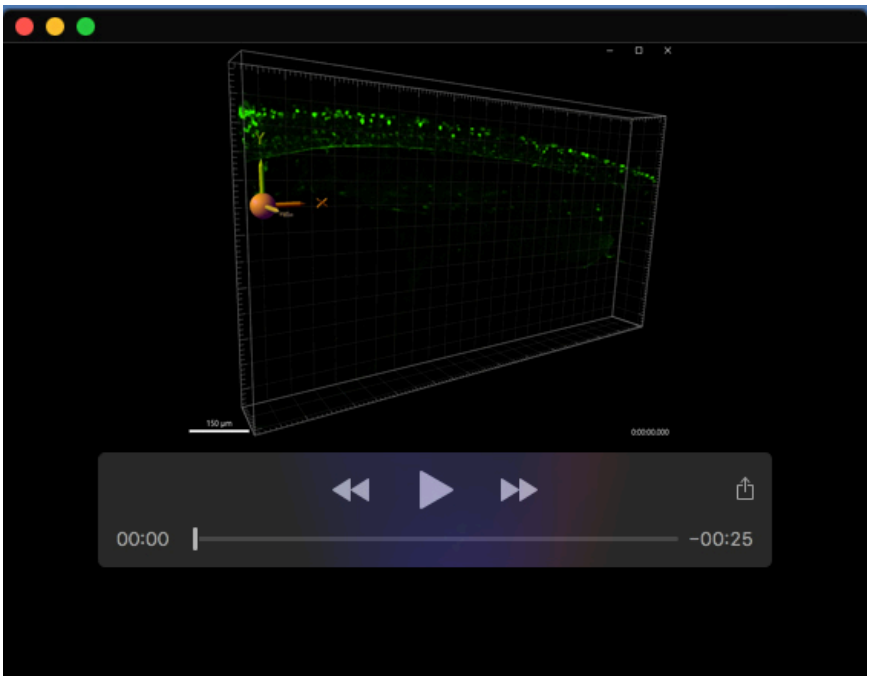

Movie 1. Enteric neural crest cells migrate posteriorly down a control zebrafish larval gut between 48-96 hpf. Lateral view of *phox2bb:*Kaede^{+} enteric neural crest cells appear in the foregut posterior to origin reference frame and continue to propagate in number as they migrate posteriorly and colonize the entire length of the gut tube.

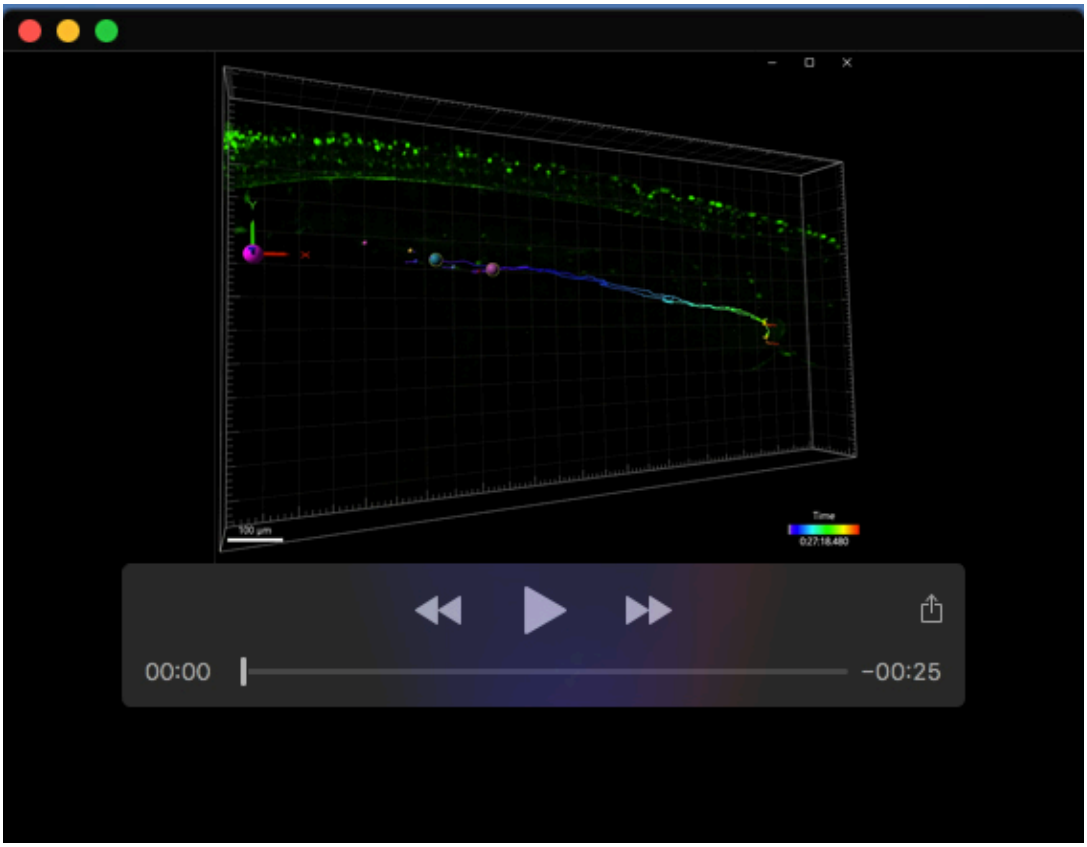

Movie 2. Enteric neural crest cells migrate posteriorly down a control zebrafish larval gut between 48-96 hpf, with IMARIS spots shown. Same movie as Movie 1 with cell spots overlaid with each individual *phox2bb:*Kaede^{+} enteric neural crest cell (color coded based on unique ID). Large turquoise and pink spots correspond to leading most (vanguard) cell in the right and left migratory cell chains, respectively. Tracks correspond to vanguard migratory track and are color coded based on time during movie.

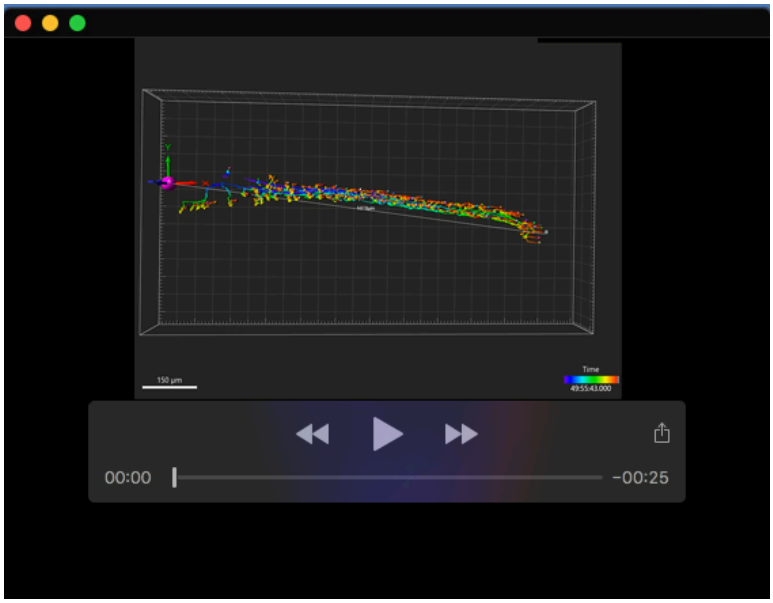

Movie 3. Animated 360° horizontal rotation of cell tracks from Figure 1D and Movie 2. Tracks color coded cold-hot for timepoints throughout time-lapse.

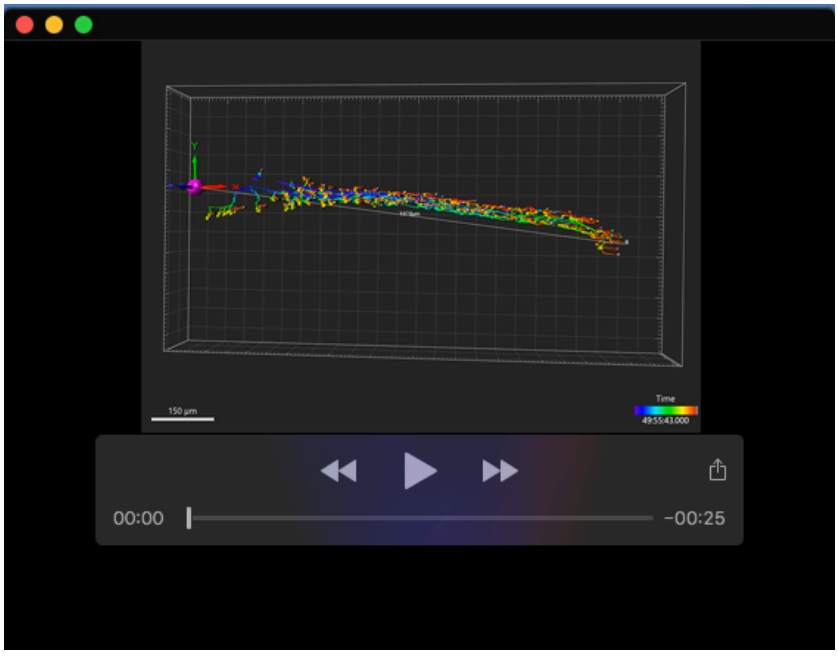

Movie 4. Animated 360° vertical rotation of cell tracks from Figure 1D and Movie 2. Tracks color coded cold-hot for timepoints throughout time-lapse.

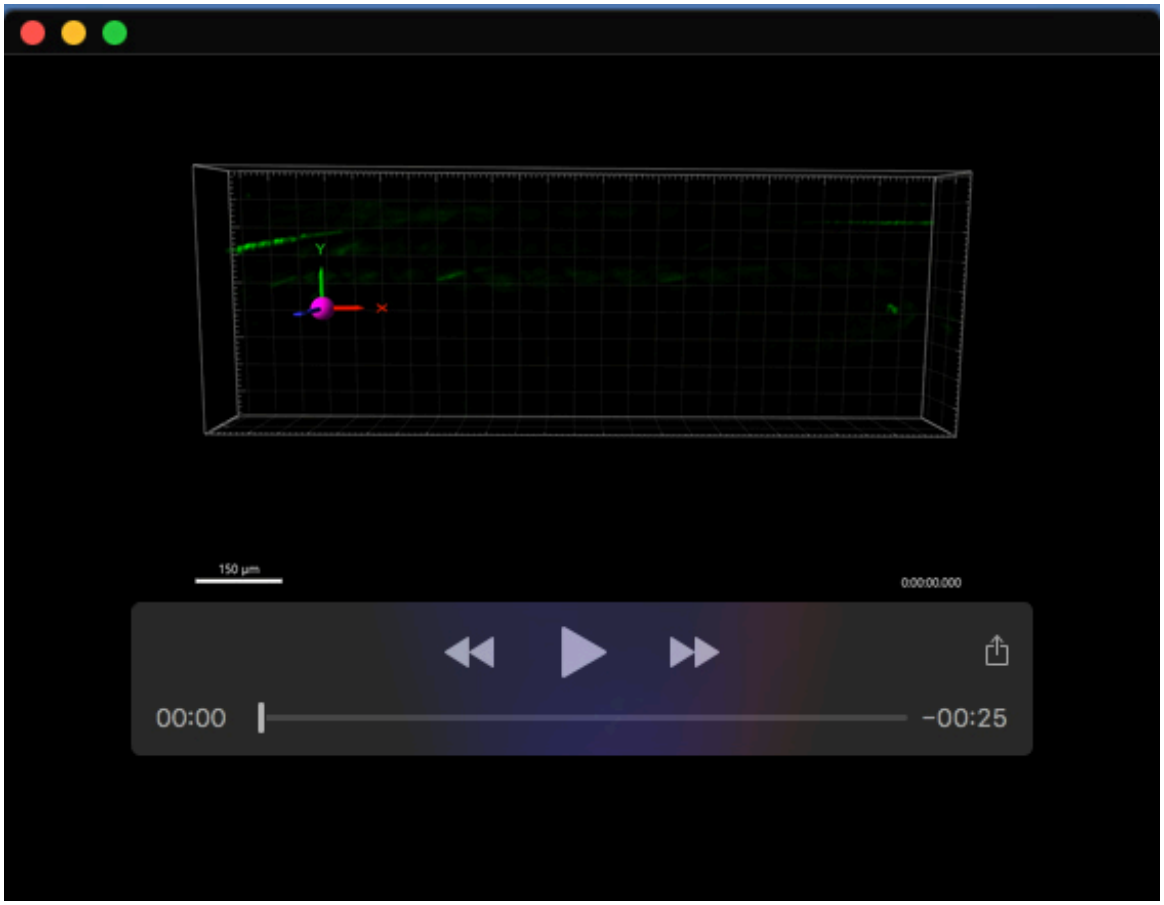

Movie 5. Enteric neural crest cells migrate posteriorly down *ret*$^{wmr1/+}$ zebrafish larval gut between 48-96 hpf. Lateral view of *phox2bb:*Kaede^{+} enteric neural crest cells appear in the foregut posterior to origin reference frame and migrate posteriorly yet fail to colonize the entire length of the gut tube.

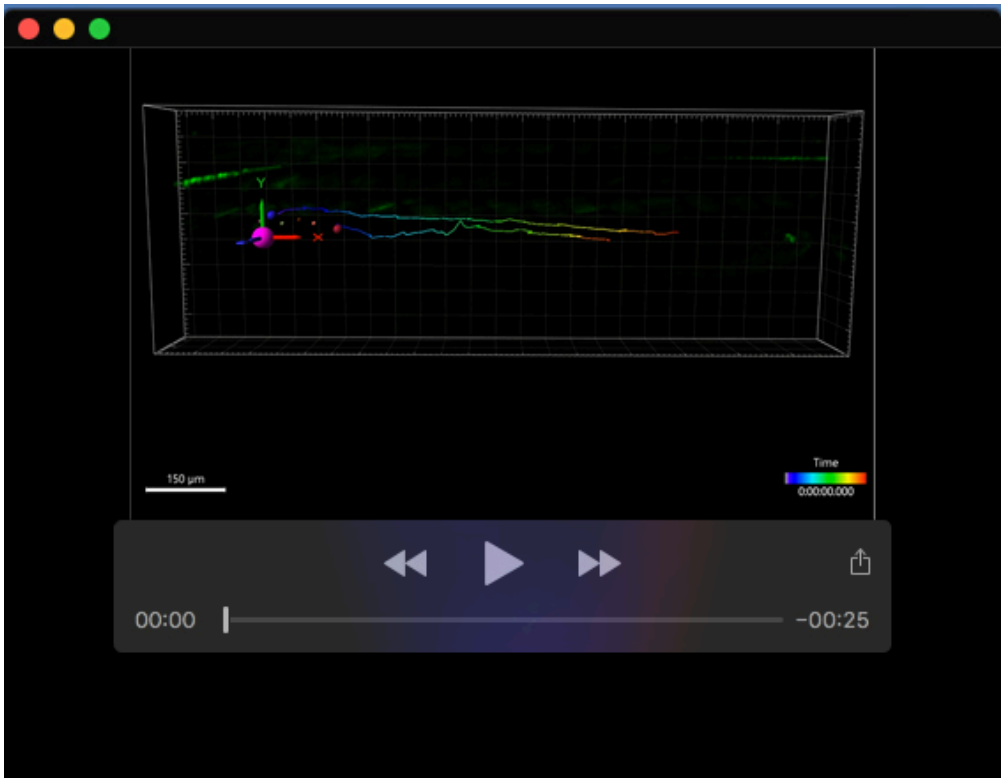

Movie 6. Enteric neural crest cells migrate posteriorly down *ret*$^{wmr1/+}$ zebrafish larval gut between 48-96 hpf, with IMARIS spots shown. Same movie as Movie 3 with cell spots overlaid with each individual *phox2bb:*Kaede^{+} enteric neural crest cell (color coded based on unique ID). Large turquoise and pink spots correspond to leading most (vanguard) cell in the right and left migratory cell chains, respectively. Tracks correspond to vanguard migratory track and are color coded based on time during movie.